Desalination and Water Treatment
www.deswater.com

doi:10.5004/dwt.2017.21031

83 (2017) 75–85
July

Removal of diclofenac from water with calcined ZnAlFe-CO_3 layered double hydroxides: Effect of contact time, concentration, pH and temperature

Rima Ghemit[a], Mokhtar Boutahala[a,*], Abdelkrim Kahoul[b]

[a]*Laboratoire de Génie des Procédés Chimiques (LGPC), Faculté de Technologie, Université Ferhat Abbas Sétif-1, 19000 Sétif, Algérie, Tel. +213-36-83-49-74, Fax +213-36-83-49-74, email: rymghemit@yahoo.fr (R. Ghemit), mboutahala@yahoo.fr (M. Boutahala)*
[b]*Laboratoire d'Energétique et d'Electrochimie du Solide (LEES), Département de Génie des Procédés, Faculté de Technologie, Université Ferhat Abbas, Sétif-1, 19000 Sétif, Algérie, email: kahoulabdelkrim@yahoo.fr (A. Kahoul)*

Received 17 October 2016; Accepted 16 June 2017

ABSTRACT

In this study, ZnAlFe-CO_3 layered double hydroxide (LDH), with a Zn to (Al+Fe) molar ratio of 2 and an Al to Fe molar ratio of 1:1, was successfully synthesized and its calcined product (ZnAlFe-C) was obtained. The prepared adsorbents ZnAlFe-CO_3 and ZnAlFe-C were characterized by FTIR, XRD, TGA/DTA and BET textural analysis. Batch sorption studies were conducted to investigate adsorption of diclofenac from water onto both adsorbents. The results show that ZnAlFe-C can be used as an effective adsorbent and its sorption capacity is higher than that of ZnAlFe-CO_3.The adsorption processes can be well described by the pseudo-second- order kinetic model. The adsorption data are fitted well with the Langmuir isotherm equation. The maximum adsorption capacity is 641.48 mg/g. The thermodynamic parameters were calculated. The negative ΔG^0 and ΔH^0 indicate that the adsorption processes are spontaneous and exothermic in nature.

Keywords: Pharmaceutical; Diclofenac; Adsorption; LDHs; Capacity

1. Introduction

The contamination of aquatic systems by pharmaceuticals and personal care products (PPCPs) is widely reported and represents a growing concern and risk for the environment and human health [1,2]. For instance, the diclofenac (DIC), one of the most common and representative PPCPs, is widely used in human medical care; it enters the aquatic environment through human excretions [3]. The removal efficiency in wastewater treatment plants (WWTPs) is very low for diclofenac and leads to surface water contamination [3,4]. Diclofenac and its metabolites are commonly detected in many countries at concentrations up to μ g L^{-1} range in sewage effluents, surface waters, and even in ground water and drinking water [4,5]. The removal of diclofenac from water resources is of vital concern to researchers worldwide.

From the literature, a number of procedures such as photodegradation [6], coagulation–flocculation [7], biodegradation [8], chlorination [9], advanced oxidation processes (AOPs) and ozonation [10,11] have been used for the removal of pharmaceutical contaminants from water. However, these methods have certain disadvantages such as high capital cost and operational costs. As an alternative, the adsorption technique can be applied to remove these kinds of effluents. Adsorption offers significant advantages over traditional treatment methods especially environmental point of view [12,13]. Although activated carbon is widely used as an adsorbent owing to its excellent adsorption abilities, its high price limits usage.

Layered double hydroxides (LDHs), commonly known as anionic clays or hydrotalcite-like compounds, are composed of positively charged brucite-like sheets and negatively charged anions in the hydrated interlayer regions. They can be represented by this general formula, $\left[M^{II}_{1-x}M^{III}_{x}(OH)_2\right]^{x+}\left(A^{n-}\right)_{\frac{x}{n}}.mH_2O$, where M^{II} and M^{III} are divalent metal cations (Mg^{2+}, Zn^{2+}, Ni^{2+}, Cu^{2+}, Ca^{2+}, etc.)

*Corresponding author.

and trivalent metal cations (Al^{3+}, Fe^{3+}, Ga^{3+}, Cr^{3+}, etc.), respectively. A^{n-} denotes exchangeable interlayer anion with negative charge *n*, *m* is the number of interlayer water and *x* is defined as the $M^{III}/(M^{II}+M^{III})$ ratio [14]. During controlled thermal decomposition, LDH progressively suffers the loss of physisorbed and interlayer water, decomposition of interlayer anions, and dehydroxylation of brucite-like sheets [15]. The calcination of these LDHs (CLDHs) produces non stoichiometric mixed metal oxides as intermediates, which are characterized by high specific surface areas, high anion exchange capacities, strong Lewis basic sites (O^{2-} species), flexible interlayer space and homogeneous dispersion of metal cations [16]. Rehydration of CLDHs leads to the reconstruction of the original layered structure, which is described as a "memory effect" [17]. As a kind of promising adsorbents, CLDHs have been widely used for the removal of contaminant anions in wastewaters, even better than their LDH precursors [16,17]. In our previous works, we demonstrated that CLDHs provided a good adsorption potential for the removal of 2.4.5-TCP [18], orange methyl [19], anionic dye Biebrich scarlet [20], CO oxidation [21] and Cr VI [22].

Here, we report on the preparation of LDHs, with Zn as divalent cation, and Al and Fe as trivalent ones following the coprecipitation method. Despite the fact that most of the previous studies have been carried out with systems with only one divalent and one trivalent cation, we have included here a system with one divalent (Zn) and two trivalent cations (Al, Fe) in the brucite-like layers. The choice of the metal ions is based on the fact that the trivalent cations Al^{3+} and Fe^{3+} are non-toxic, stable, cheap, friendly to the environment in comparison with other trivalent cations (Ni, Co, Mn, Cr). As the ionic radii of Al^{+3} (0.50 Å) and Fe^{+3} (0.64 Å) are similar than that of zinc ion (0.74 Å) (Table 1) [14], these ions are accommodated in the holes of close packed configuration of OH groups in the brucite-like layers.

The present study aims to evaluate the potential adsorption capacity of DIC onto ZnAlFe-C in an aqueous medium as a function of various adsorption parameters, such as pH, contact time, initial concentration, adsorbent dosage and coexisting ions. The equilibrium isotherm and kinetic model of the adsorption process were also studied to evaluate the viability and effectiveness of the process. According to the literature review, there are not many studies focused on the elimination of emerging contaminants like diclofenac (DIC) by ZnAlFe LDH.

Table 1
Ionic radius of divalent and trivalent cations involved in LDHs materials

MII	Ionic radius (Å)	MIII	Ionic radius (Å)
Mg	0.65	Al	0.50
Cu	0.69	Ga	0.62
Ni	0.72	Ni	0.62
Co	0.74	Co	0.63
Zn	0.74	Fe	0.64
Fe	0.76	Mn	0.66
Mn	0.80	Cr	0.69
Ca	0.98	In	0.81

2. Experimental

2.1. Materials

Reagent grade (99%) NaCl, HCl, NaOH, $AlCl_3{\cdot}9H_2O$, $ZnCl_2{\cdot}6H_2O$, $FeCl_3{\cdot}9H_2O$ were supplied by Sigma-Aldrich. The adsorbate diclofenac sodium (abbreviated as DIC) (water solubility > 2000 mg/L, pKa = 4.1, molecular weight = 318.14, boiling point = 412°C) was also purchased from Sigma-Aldrich.

2.2. Synthesis of ZnAlFe-layered double hydroxide

ZnAlFe-CO_3 with $Zn^{+2}/(Al^{3+}+Fe^{3+})$ molar ratio of 2 was prepared by coprecipitation at a fixed pH 10 ± 0.5, following the method described by Reichle [23]. A metal salt solution containing $ZnCl_2{\cdot}6H_2O$ (44.97 g), $AlCl_3{\cdot}9H_2O$ (19.92 g) and $FeCl_3{\cdot}9H_2O$ (13.37 g) was added drop wise to a vigorously stirred NaOH 2 M, Na_2CO_3 1 M aqueous solution. The resulting slurry was kept at 65°C for 24 h, centrifuged, washed with deionized water until obtaining a Cl^- free ZnAlFe-CO_3. Finally, the product was dried for 18 h at 80°C, ground and passed through a 100-mesh sieve. A fraction of the resulting material (ZnAlFe-CO_3) was calcined in a muffle furnace at 500°C for 5h; the solid obtained was denominated ZnAl-Fe-C. The calcined product was directly characterized and investigated in adsorption experiments.

2.3. Characterization of samples

X-ray diffraction (XRD) analysis of the LDH samples was conducted using a Philips ®X-Pert diffractometer with Cu Kα radiation. The software used was XPOWDER®.

FTIR study was carried out using a FTIR spectrophotometer JASCO 6200, with a software SPECTRA MANAGER v2. FTIR spectra were recorded in the range of 400–4000 cm^{-1} at 0.5 cm^{-1} resolution using KBr pellets.

Thermogravimetric analyses were performed on a METTLER TOLEDO mod. TGA/DSC1 with a FRS5 sensor and a microbalance Mettler-Toledo GMBH (precision 0. 1 µg). Samples were heated in a platinum crucible between 10 and 950°C at a heating rate of 10°C/min under a stream of nitrogen.

Nitrogen gas adsorption-desorption isotherms were measured using a Micromeritics Tristar 3000 instrument at 77K. The measurements were made after degassing the samples under vacuum at 200°C for 3h. The specific surface areas were determined according to the BET method at the relative pressure in the range 0.05–0.35 [24]. The total pore volumes of micro and mesopores were directly determined from the nitrogen adsorption at $P/P_0 = 0.98$. The pore size distribution is calculated using the Barret-Joyner-Haleda (BJH) method using the desorption isotherm [25].

The point of zero charge (pH_{pzc}) of LDHs used for the adsorption is determined using solid to liquid ratio of 1:1.000. For this, 0.1 mg of LDHs is added to 100 mL of water with varying pH from 4 to 12 and stirring for 24 h. The final pH value is plotted against initial pH of the solution [19].

2.4. Adsorption experiments

It should be noted that the kinetic study for ZnAlFe-CO_3 was not included in this work due to the lower adsorption capacity of this material compared to that of ZnAlFe-C.

The effect of pH on DIC adsorption onto ZnAlFe-C was studied under initial solution pHs ranging from 4 to 10. The initial DIC concentration in the studied solutions was 50 mg/L and the quantity of ZnAlFe-C was 50 mg. The volume and agitation speed were 50 mL and 200 rpm, respectively. All studies were performed by stirring the mixtures at 25 ± 1°C. The initial solution pH was adjusted with HCl or NaOH.

The effect of adsorbent dosage was performed at pH 6.7 and room temperature 25 ± 1°C for 3 h. The initial DIC concentration was 50 mg/L and the adsorbent dosage range of ZnAlFe-C was 5–200 mg.

The effect of the ionic strength was evaluated by varying the concentration of the ionic solutions (NaCl, KNO_3, Na_2SO_4, K_3PO_4 and Na_2CO_3) from 0 to 1000 mg/L. Every solution was mixed with 50 mL of 50 mg/L DIC solution and 50 mg of ZnAlFe-C at pH = 6.7 and T = 25 ± 1°C.

Kinetic batch tests were carried out with 1000 mg/L of the DIC stock solution diluted to 5–600 mg/L. For this, a known amount of ZnAlFe-C (20 mg) was dispersed in 20 mL of DIC solution at pH = 6.7 and T = 25 ± 1°C. After each contact time, a sample was taken and centrifuged. The amount of DIC adsorbed was derived from the initial and final concentrations of DIC in the liquid phases.

For the adsorption isotherm, 20 mL of a DIC solution with initial concentrations ranging from 5 to 1000 mg/L was mixed with a constant amount of ZnAlFe-C (20 mg). The dispersions were shaken at a temperature of 25 ± 1°C, a free pH (i.e. pH > pKa (DIC)) and under an agitation speed of 200 rpm. To reach equilibrium, the dispersions were maintained at a constant pH for 3 h. After completing each adsorption experiment, the solid phase was separated from the liquid phase by centrifugation at 5000 rpm for 15 min. The equilibrium supernatant liquid concentrations were determined at the wavelength of maximum absorption (276 nm) using a Shimadzu UV–Vis 1700 spectrometer. The amounts adsorbed at equilibrium (q_e) and at any time (q_t) were calculated using the following equation:

$$q_{e,t} = \left[\frac{(C_0 - C_{e,t})}{m}\right] \times V \quad (1)$$

where $q_{e,t}$ (mg/g) is the adsorbed quantity at equilibrium (q_e) or at any time (q_t), C_0 (mg/L) is the initial DIC concentration, $C_{e,t}$ (mg/g) is the DIC concentration at equilibrium (C_e) or any time (C_t), V(L) is the volume of the solution, and m(g) is the mass of the ZnAlFe-C adsorbent.

For the regeneration study, a portion of 100 mg ZnAlFe-C adsorbent was placed in 100 mL of 100 mg/L diclofenac solution and shaken for 3 h at room temperature. After adsorption, the sample (ZnAlFe-CDIC) was filtered, washed with water and then dried at 50°C. To desorb the DIC, the ZnAlFe-CDIC sample was treated for 3 h using ethanol, then, the sample (ZnAlFe-C) was separated by filtration, washed and dried. The latter sample (ZnAlFe-C) was then subjected repeatedly to successive adsorption-desorption cycles.

3. Results and discussion

3.1. Characterizations of adsorbents

The XRD patterns of ZnAlFe-CO_3, ZnAlFe-C and ZnAlFe-CDIC (after adsorption of DIC) are shown in Fig. 1. As can be seen, before calcination, the synthesized ZnAlFe-CO_3 (Fig. 1a), shows typical hydrotalcite ($HTCO_3$) structure with sharp and symmetric reflections for (003), (006) as well as wide and asymmetric reflections for (012), (015) and (018) planes. All of these reflections are the characteristic of hydrotalcite-like compounds [14]. For this material, the interlayer space (d) calculated from the Bragg equation ($n\lambda = 2d \sin\theta$) is 7.42 Å, which can be assigned to the intercalation of carbonate ions between the inorganic lamellae [26,27]. After calcination, the characteristic reflections of LDH disappeared and the hydrotalcite phase was transformed into an amorphous structure, due to dehydration and decarbonation according to the modification that appears in Fig. 1b. Only a few diffused peaks observed at 31.62° (2.82 Å) and 35.11° (2.55 Å) are attributed to mixed oxides [28]. However, reconstruction of the layered structure (Fig. 1c) has been observed to take place after diclofenac adsorption giving a material with a basal spacing of 7.5 Å by the "memory effect" of CLDHs [29]. The basal spacing of d_{003} is almost the same of that of the LDH precursor, which indicates that there are a few DIC anions between the interlayer, due to the strong interaction between CO_3^{2-} and the layers. XRD patterns indicate a little increase in basal spacing from d = 7.42 Å to 7.5 Å. Therefore, the DIC adsorption occurred mainly on the external surface of the material.

The FTIR spectra of ZnAlFe-CO_3, ZnAlFe-CDIC and DIC are depicted in Fig. 2. The spectrum of the ZnAlFe-CO_3 (Fig. 2a) shows characteristic bands of hydrotalcite-like phases with CO_3 as the counter anion [29]. The bands at 3,456 and 1,649 cm^{-1} are attributed respectively to the O–H stretching and bending vibrations of hydroxyl groups and water molecules [30]. The band observed around 1,353 cm^{-1} is assigned to a vibrational mode of the CO_3^{2-} anions [31]. The absorption bands below 1,000 cm^{-1} are interpreted as the lattice vibration mode of M–O and M–OH with M representing Zn, Al or Fe [32–34]. FTIR spectrum of DIC (Fig. 2c) shows one peak at 746 cm^{-1}, attributed to C–Cl stretching and absorption bands at 1,453 and 1,283 cm^{-1} resulted from C–N stretching. The peaks at 1,504 and 1,576 cm^{-1} resulted

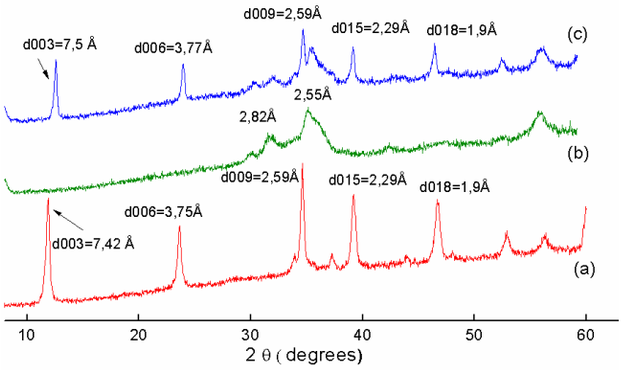

Fig. 1. X-ray diffractograms of the ZnAlFe-CO_3 (a), ZnAlFe-C (b) and ZnAlFe-CDIC (c).

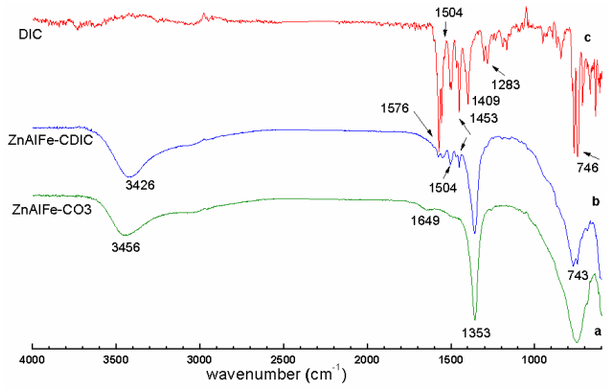

Fig. 2. FTIR spectra of the ZnAlFe-CO_3 (a), ZnAlFe-CDIC (b) and DIC (c).

from C=C and C=O stretching of the carboxylate functional group, respectively [35]. The FTIR spectrum of the ZnAlFe-CDIC in Fig. 2b exhibits new absorption bands at 1,576 cm^{-1} and 1,504 cm^{-1} corresponding to the asymmetric and symmetric stretching vibrations of the carboxylate group (COO^-) of diclofenac. These bands confirm that the DIC molecules are adsorbed onto the material.

The differential thermal analysis (DTA) and thermogravimetric analysis (TGA) curves are shown in Fig. 3. DTA thermogram of the ZnAlFe-CO_3 present in Fig. 3a displays two prominent endothermic peaks (at 186°C and at 234°C), both assigned to the elimination of water and CO_2, respectively [29]. Two weight loss stages were observed for ZnAlFe-CO_3 in the TGA curve; coinciding with the two endothermic peaks in the DTA profiles. The first weight loss at 186°C was ascribed to the loss of physically adsorbed and interlayer water. The second one in the temperature range from 200 to 400°C could be attributed to removal of carbonate anions in the interlayer and water molecules from condensation of hydroxyl groups from brucite-like layers [33], leading , thus, to the destruction of hydrotalcite structure and the formation of an amorphous metastable mixed oxides $M^{II}_xM^{III}_yO_z$ [34]. The total weight loss of the pure samples in the temperature range up to 600°C is approximately 28%, which corresponds to the sum of water and carbonate contents. Fig. 3b shows three weight losses for ZnAlFe-CDIC at 80, 193 and 533°C. The weight loss 3% from 30 to 100°C is due to the removal of surface physisorbed water molecules. The second weight loss 10% in the range of 100-250°C corresponds to the removal of water molecules from the intercalated structure. The last weight loss (533°C) is mainly attributed to the decomposition of the intercalated DIC ions under air atmosphere, accompanying with the formation of mixed oxides [35].

The N_2 adsorption-desorption isotherms of ZnAlFe-CO_3 and ZnAlFe-C are presented in Fig. 4. The inset shows the pore size distributions (PSD) determined by the Barret-Joyner-Halenda (BJH) analysis using the adsorption data. The isotherms of these samples are typical of mesoporous structures and are classified as type II on the basis of IUPAC recommendations. These isotherms also exhibit an H3 type hysteresis at high relative pressure, which is typical for aggregates of plate-like particles giving rise to slit-

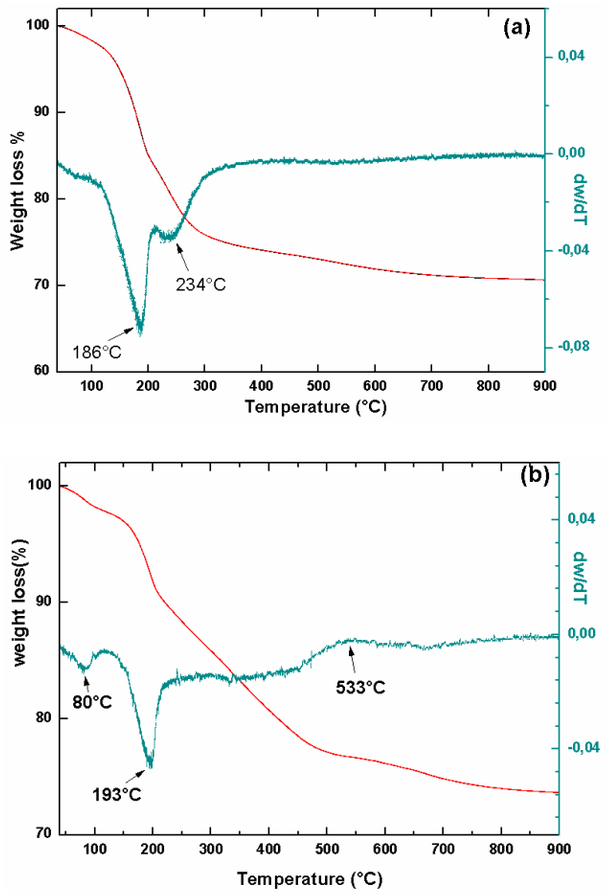

Fig. 3. TGA and DTA results of the ZnAlFe-CO_3 (a) and ZnAlFe-CDIC (b).

shaped pores [36]. This kind of hysteresis is typical for the presence of open large pores, which allow easy diffusion of the reactants through the materials. As seen from the inset in Fig. 4, the PSD curves are quite broad and monomodal with small mesopores. The peak pores are located at ca. 80 Å and 120 Å for ZnAlFe–CO_3 and ZnAlFe–C, respectively. The smaller mesopores reflect the presence of pores within nanosheets, while larger mesopores can be associated to the pores formed between stacked nanosheets [36]. The specific surface area of the ZnAlFe–CO_3 increased from 53.2 to 79.0 m^2/ g and the pore volume from 0.32 to 0.49 cm^3/g by heating at 500°C. The removal of water and carbon dioxide during calcination can lead to the formation of channels and pores [37], which are accessible to the nitrogen molecules and could increase the specific surface area of ZnAlFe–C.

The point of zero charge (pHpzc) of the adsorbent was determined by the pH drift method. A plot of the final pH (pH_f) against initial pH (pH_i) was done (figure not shown). The pHpzc value obtained for ZnAlFe-CO_3 was 7.3 and 7.5 for ZnAlFe-C. Under the pHzpc, the surface of ZnAlFe-C was positively charged and thus a high efficacy in removing negatively charged species from aqueous solution. While this material acquires a negative charge when solution pH is above the pH_{PZC}.

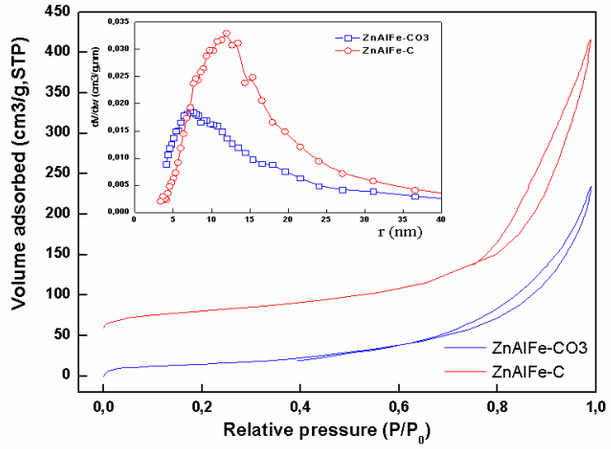

Fig. 4. N_2 adsorption/desorption isotherms of ZnAlFe-CO_3 and ZnAlFe-C. Inset shows the pore size distribution of the materials.

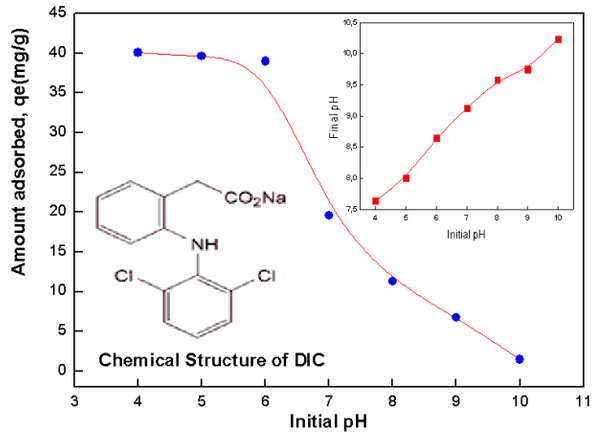

Fig. 5. Effect of the pH for the equilibrium adsorption data of DIC on the ZnAlFe-C.

3.2. Diclofenac adsorption results

3.2.1. Effect of initial pH

Solution pH not only affects the surface charge of adsorbent but also influences the pollutant species in solution by controlling their electrostatic interaction. The variation of adsorption onto the ZnAlFe-C was investigated in a pH range 4–10 using HCl or NaOH. The effect of pH on DIC removal was studied with an adsorption time of 180 min, which was found to be enough to ensure the equilibrium. Fig. 5 shows the effect of the solution pH on the removal efficiency of DIC by the ZnAlFe-C. The inset shows the final pH against initial pH. The removal of diclofenac decreased rapidly with increasing pH. The isoelectric point (pHpzc) of the ZnAlFe-C was measured to be 7.5, indicating that the adsorbent surface was negatively charged at pH above 7.5. Since the pKa of DIC was 4.1, more anionic DIC species were present in the solution with increasing pH. Therefore, the electrostatic repulsion between DIC and ZnAlFe-C increased with increasing solution pH, leading to a rapid decrease of the removal efficiency. In addition, the competitive adsorption of OH^- ions can also result in a decrease in adsorption capacity. Similar results have been previously reported for the sorption of DIC from aqueous solutions by carbon nanotubes/alumina hybrid (CNTS/Al_2O_3) [38,39].

3.2.2. Dosage effect of the adsorbent

Adsorbent dose is an important parameter in the determination of adsorption capacity. The results (Fig. 6.) show that the removal percentage increases with increasing adsorbent dose up to 50 mg and q_e amount adsorbed (mg/g) decreases with an increase in adsorbent dose from 5 to 200 mg. This can be interpreted as an increase in the adsorbent specific surface area and a porous structure of ZnAlFe-C providing more adsorptions sites that result in a higher removal percentage [40].

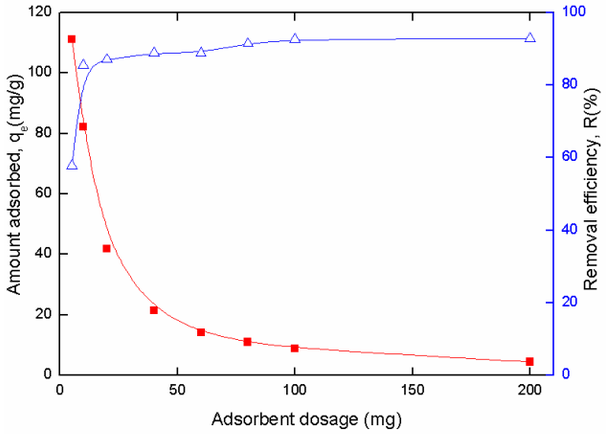

Fig. 6. Dosage effect on adsorption of DIC on ZnAlFe-C.

3.2.3. Effects of co-existing anions

In practice, natural water contains multiple anions, which can compete for adsorption sites and lead to the reduction of diclofenac removal. The effect of co-existing anions like, Cl^-, NO_3^-, CO_3^{-2}, SO_4^{-2}, PO_4^{-3}, was studied and the results are shown in Fig. 7. It was observed that the DIC adsorption capacity decreased significantly when other anions co-existed, especially when, CO_3^{-2}, SO_4^{-2}, PO_4^{-3} were present. The effect of co-existing anions on DIC adsorption decreased in the order: CO_3^{-2} > PO_4^{-3} > SO_4^{-2} > Cl^- > NO_3^-. This effect towards adsorption may be due to their affinity towards ZnAlFe-C. It has been reported [19,20] that the adsorptive tendency of multicharge anions is higher than that of monovalent anions. Therefore the anion with higher charge density has greater effect on DIC adsorption onto ZnAlFe-C [41].

3.2.4. Effect of concentration on ZnAlFe-C

The effect of DIC initial concentrations (5–600 mg/L) on ZnAlFe-C is presented in Fig. 8. The adsorption uptake

of DIC gradually increases when the concentration increases. It is evident from the figure that the DIC removal was rapid in the initial stages of contact time and reached already equilibrium after 120 min for all concentrations. The rapid adsorption at the initial contact time can be attributed to the abundant availability of active sites on the adsorbent surfaces. After occupancy of these sites, the adsorption became less efficient. The superior adsorption capacity at high initial concentration is perhaps due to the generation of significant driving forces caused by a pressure gradient [42].

3.2.5. Kinetic study

To investigate the mechanism of diclofenac adsorption, two kinetic models were considered, pseudo-first-order, and pseudo-second-order models. Those models were the most commonly used to describe the adsorption of organic and inorganic pollutants onto solid adsorbents. The nonlinear form of Lagergren pseudo-first-order model can be expressed as

$$q_t = q_e(1-\exp^{-k_1 t}) \tag{2}$$

where q_e and q_t are the adsorption capacities at equilibrium and at time t (min), respectively, and k_1 (L/min) is the rate constant of first-order adsorption.

The nonlinear form of pseudo-second-order kinetic model can be expressed as [44]:

$$q_t = \frac{q_e^2 k_2 t}{1+q_e k_2 t} \tag{3}$$

where k_2 (g/mg·min) is the rate constant for the second-order kinetic model.

The pseudo-first-order and pseudo-second-order kinetic parameters determined along with the determination of coefficient (R^2) are presented in Table 2. The R^2 can be determined by the following equation [42]:

$$R^2 = 1 - \frac{\sum_{n=1}^{n}\left(q_{t.\exp.n} - q_{t.cal.n}\right)^2}{\sum_{n=1}^{n}\left(q_{t.\exp.n} - \overline{q_{t.\exp.n}}\right)^2} \tag{4}$$

where $q_{t\ exp}$ and $q_{t\ cal}$ are the experimental adsorption capacity at time t and the calculated adsorption capacity at time t from the models, respectively, n is the number of observations.

According to Table 2 and the nonlinear fitted plots presented in Fig. 8, the adsorption kinetics of DIC onto ZnAlFe-C is better described by the pseudo second-order kinetic model than the pseudo first-order one at all initial concentrations because of the high R^2 values. Additionally, the experimental values of adsorption capacity (q_{exp}) are very close to the calculated values of adsorption capacity (q_{cal}). Several authors showed the successful application of pseudo-second-order model for the representation of experimental kinetics data of DIC adsorption on different adsorbents [45–47].

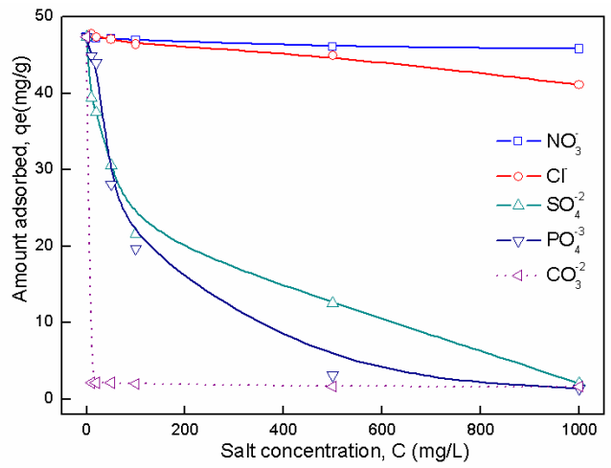

Fig. 7. Effect of coexisting ion (Cl^-, NO_3^-, SO_4^{-2}, PO_4^{-3}, CO_3^{-2}) on the adsorption performance of ZnAlFe-C (pH = 6.7, m = 50 mg, V = 50 mL, C_o = 50 mg/L, T = 25±1°C).

Table 2
Kinetic non-linear models parameters for DIC adsorption by ZnAlFe-C

		Pseudo-first order			Pseudo-second order		
C_o(mg/L)	q_{exp}	k_1*10^{+2}	q_e	R^2	k_2*10^{+3}	q_e	R^2
5	2.5	1.55	2.7	0.993	3.9	3.5	0.994
10	5.4	6.3	4.9	0.918	18.4	5.4	0.973
15	13.2	5.3	12.6	0.949	5.9	13.9	0.987
20	16.6	3.9	16.0	0.972	3.0	18.1	0.990
50	47.2	11.3	45.3	0,987	4.3	48.4	0.991
100	96.9	2.3	97.2	0,972	0.2	118.1	0.978
200	197.2	5.6	192.5	0,987	0.4	211.9	0.989
400	401.0	16.1	398.9	0,991	0.9	415.6	0.997
600	538.9	4.0	548.0	0,982	0.08	624.2	0.970

k_1 (min^{-1}), k_2 (g/mg·min), q_e (mg/g), q_{exp} (mg/g).

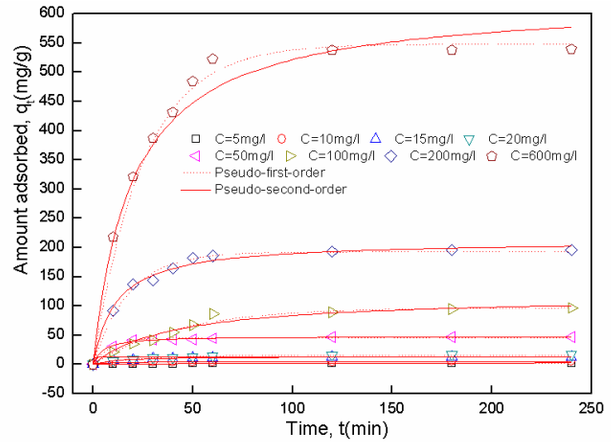

Fig. 8. Kinetic adsorption data for Diclofenac onto the ZnAlFe-C at concentration (5–600 mg/ L) (pH = 6.7, m = 50 mg, V = 50 mL, T = 25±1°C).

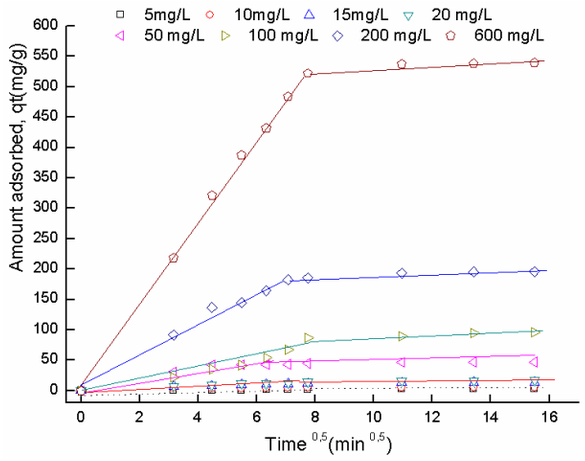

Fig. 9. Intraparticle diffusion model of the adsorption of Diclofenac onto ZnAlFe-C.

3.2.6. Adsorption mechanism

Intraparticle diffusion is a transport process involving movement of species from the solution bulk to the solid phase. In a well stirred batch adsorption system, the intraparticle diffusion model is used to describe the adsorption process occurring on a porous adsorbent. A plot that expresses the amount of adsorbate adsorbed, q_t (mg g^{-1}) as a function of the square root of the time, gives the rate constant by calculating the plot slope. This model can be described by the following equation [48]:

$$q_t = k_{id}\sqrt{t} + C \tag{5}$$

where k_{id} (mg·g^{-1} $h^{-0.5}$) and C are diffusion coefficient and intraparticle diffusion constant, respectively. C is directly proportional to the thickness of the boundary layer.

According to this model, the plots (Fig. 9) are nonlinear for the whole range of studied concentrations, indicating that intraparticle diffusion is not the only rate-limiting step, but an other process may also be involved in the adsorption process. Two different sharp stages are clearly observed in Fig. 9. The first stage, including the adsorption period from 0 to 60 min ($t^{1/2} < 8.0$), describes the instant adsorption stage where DIC adsorption rate is high because of a large surface area and a low competition between the diclofenac molecules. The second part, ranging from 60 to 250 min ($8.0 < t^{1/2}) < 16$), is attributed to the low adsorption stage caused by the low concentration gradients, producing the equilibrium condition. The values of k_{id} were determined from the slopes of the linear plots and presented in Table 3.

The Film diffusion model was also used in this study to investigate if transport of DIC from the liquid phase up to the solid phase boundary also plays a role in the adsorption process equation [49]:

$$-\ln\left(1-\frac{q_t}{q_e}\right) = K_{fd}t \tag{6}$$

where K_{fd} is the liquid film diffusion constant. Table 3 summarizes the intraparticle diffusion and film diffusion parameters for DIC adsorption on ZnAlFe-C at different initial DIC concentrations. The adsorption process follows the film mechanism when the plots of $\ln\left(1-\frac{q_t}{q_e}\right)$ vs. t (figure not shown) at different initial concentrations are linear or non linear but do not pass through the origin, thereby explaining the influence of film diffusion mechanism on the adsorption rate. Likewise, by comparing the data presented in Table 3, the R^2 values for the intraparticle diffusion were higher than those of the film diffusion model. This observation suggested that intraparticle diffusion mainly controlled the rate of DIC adsorption on ZnAlFe-C under the studied conditions.

3.2.7. Adsorption isotherm

Adsorption isotherms describe how adsorbates interact with adsorbents in an adsorption system. Moreover, by isotherm analysis, the adsorption capacity of the adsorbent, which is an important parameter in the industrial design for adsorption process, was predicted. Adsorption isotherm for DIC retention by ZnAlFe-C is presented in Fig. 10. This isotherm indicates that DIC has a high affinity for ZnAlFe-C surface, particularly at low concentrations. Isotherm was characteristic of a typical L-type adsorption reaction that represented a system where the adsorbate was strongly attracted by the adsorbent. The sorption (q_e) increased with increasing equilibrium concentration (C_e), and gradually approached the maximum sorption capacities with a DIC equilibrium concentration of 250 mg/L. In this study, Langmuir (Eq. (7)) [50], Freundlich (Eq. (8)) [51] and Sips (Eq. (9)) [52] isotherm models were used to describe the adsorption isotherm and to study the relationship between the amounts of DIC adsorbed (q_e) and its equilibrium concentration in the solution at 25°C.

$$q_e = \frac{q_m K_L C_e}{1 + K_L C_e} \tag{7}$$

Table 3
Intraparticle diffusion and film diffusion parameters

DIC con. (mg/L)	Intraparticle diffusion model				Film diffusion model	
Parameters	Step 1		Step2			
	K_{id}*10^{+1}	R^2	K_{id}*10^{+1}	R^2	K_{fd}*10^{+3}	R^2
5	2.3	0.907	1.13	0.859	5.7	0.893
10	5.7	0.905	1.02	0.891	20.0	0.956
15	14.5	0.941	2.22	0.842	12.0	0.857
20	18.0	0.975	2.8	0.768	9.7	0.818
50	55.7	0.809	2.9	0.608	11.7	0.643
100	104.3	0.919	13.7	0.959	7.0	0.780
200	242.3	0.971	13.1	0.792	9.4	0.640
600	718.3	0.955	21.3	0.636	7.4	0.580

k_{id} (mg/g min$^{0.5}$), k_{fd} (min^{-1})

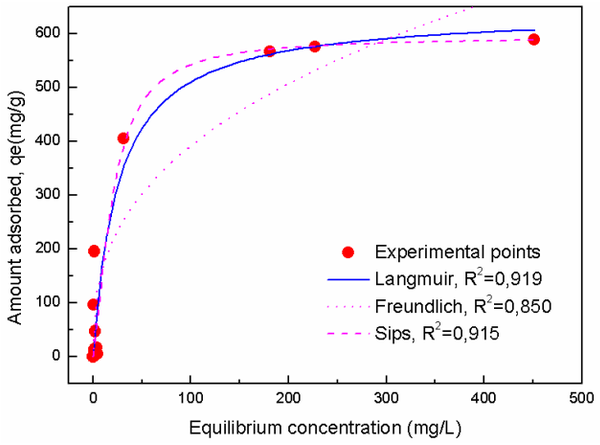

Fig. 10. Equilibrium adsorption data for Diclofenac onto ZnAl-Fe-C (pH = 6.7, m = 50 mg, V = 50 mL, T = 25±1°C).

$$q_e = K_F C_e^{\frac{1}{n}} \tag{8}$$

$$q_e = \frac{q_s K_s C_e^{\frac{1}{m}}}{1 + K_s C_e^{\frac{1}{m}}} \tag{9}$$

where q_e (mg·g^{-1}) and C_e (mg·L^{-1}) represent, respectively, the amount of DIC adsorbed and DIC concentration at equilibrium. q_m, K_L, q_s, K_s are the Langmuir and Sips constants indicating the maximum monolayer capacity of solid and strength or affinity of solid toward the sorbing species DIC, respectively. On the other hand, the K_F and $1/n$ represent the Freundlich constants, referring to the maximum sorption capacity and adsorption intensity, respectively, $1/m$ is Sips constant related to energy of adsorption, parameter m could be regarded as the Sips parameter characterizing the system heterogeneity.

Adsorption isotherm data were fitted to the above-mentioned isotherm equations by nonlinear regression analysis, using Microcal origin (8) software. The isotherm equation applicability was based on a comparison of the determination coefficient (R^2). The best isotherm model is identified through the value of R^2 given by the following equation:

$$R^2 = 1 - \frac{\sum_{n=1}^{n}\left(q_{e,\exp,n} - q_{e,cal,n}\right)^2}{\sum_{n=1}^{n}\left(q_{e,\exp,n} - \overline{q_{e,\exp,n}}\right)^2} \tag{10}$$

Table 4
Freundlich, Langmuir and Sips parameters for the DIC adsorption

Langmuir		Freundlich		Sips	
q_m (mg/g)	641.4	K_F	70.8	q_s (mg/g)	594.3
				K_s*10^{+2}	1.3
K_L*10^{+2}	3.91	$1/n$	0.37	m	0.69
R^2	0.919	R^2	0.850	R^2	0.915

The calculated constants of the three isotherm equations, along with R^2 values, are presented in Table 4. The table indicates that the Langmuir equation gives the best satisfactory fitting to the adsorption isotherms of the DIC adsorption onto the ZnAlFe-C sample with higher correlation coefficient (0.919) than those related to Sips (0.915) and Freundlich (0.850) models, indicating the homogenous nature of the surface and the formation of a monolayer of DIC on the surface of the adsorbent. The Langmuir maximum adsorption capacity was 641.4, 8 mg/g. It is worth noting that Sips isotherm model might be useful to fit the data for obtaining a high determination coefficient (R^2= 0.915), but this model does not describe the DIC adsorption on ZnAlFe-C as closely as the Langmuir model. However, the calculated value of the Freundlich model parameter $1/n$, which is in the interval from 0 to 1, suggests that the adsorption of DIC onto ZnAlFe-C is favorable. The result obtained coincides with the works carried out by previous researchers, which reported that the Langmuir model provided a better fit than the Freundlich and Sips models for diclofenac adsorption on various adsorbents, such as functionalized silica-based porous materials

Table 5
Comparison of monolayer equilibrium capacity for DIC with other adsorbents

Adsorbents	C_0 (mg/L)	q_m(mg/g)	Ref.
ZnAlFe	5–1000 mg/L	641.4	This study
Activated carbon from olive stones	5–60 mg/L	11.0	55
Pillared clay	50–1000 mg/L	100	56
Granular carbon nanotubes/alumina hybrid (CNTs/Al_2O_3)	2.47 mg/L–29.6 mg/L	107	38
Organo-K10 montmorillonite	10–500 mg/L	55.5	47
Activated carbon from COCOA SHELL	10–300 mg/L	63	57
Zeolite modified with cetylpyridinium chloride	50–500 mg/L	160	58
Activated carbon (commercial)	1–140 mg/L	76	5
UiO-66	1–140 mg/L	189	5
18%SO_3H-UiO-66	1–140 mg/L	263	5
Modified diatomite	1–4 mg/mL	390.02	59
MIEX resin	10–60 mg/L	322.31	41

[53], activated carbon [46], and organo-K10 montmorillonite [47]. The adsorption capacity of DIC in this study was compared to other sorbents and reported in Table 5. The adsorption capacity is higher than those accounted by several adsorbents. According to these results, we presume that ZnAlFe-C is a promising material for the removal of contaminants in wastewaters.

3.2.8. Effect of temperature on adsorption and thermodynamic studies

The effect of temperature of the DIC adsorption on the ZnAlFe-C was investigated under isothermal conditions in the temperature range 25–55°C. The DIC adsorption capacity onto ZnAlFe-C decreases with increasing temperature, suggesting that the adsorption reaction is exothermic. The change in standard free energy ($\Delta G°$), enthalpy ($\Delta H°$) and entropy ($\Delta S°$) of adsorption were calculated using Eqs. (11) and (12) (Van't Hoff equation):

$$\Delta G° = -RTlnK_c \quad (11)$$

$$lnK_c = \frac{-\Delta H^0}{RT} + \frac{\Delta S^0}{R} \quad (12)$$

where R is the gas constant, T the temperature in K and K_c is the equilibrium constant (L/mg). The slope and intercept of the Van't Hoff plot (Fig. not shown) is equal to $-\Delta H°/R$ and $\Delta S°/R$, respectively. Thermodynamic parameters obtained are summarized in Table 6. The $\Delta G°$ values at different temperatures are negative and decrease with an increase in temperature, indicating that the adsorption process is spontaneous and inversely proportional to the temperature. Negative values of $\Delta H°$ indicate the exothermic nature of the process. The standard enthalpy change, lower than the value of 40 kJ/mol, indicates the physical nature of adsorption. The negative value of $\Delta S°$ suggests that the adsorption process involves an associative mechanism and that there is no significant change occurring in the internal structures of the adsorbent during the adsorption process.

Table 6
Thermodynamics adsorption parameters for DIC on ZnAlFe-CO_3

ΔH (kJ/mol)	ΔS (J/mol)	ΔG (kJ/mol)			
–32.3	–41.5	283	296	303	313
		–20.53	–19.99	–19.70	–19.28

3.2.9. Adsorbent recycling

The adsorption-desorption cycles were investigated to determine the reusability of the sample for the adsorptive removal of diclofenac from aquatic environment. The ZnAlFe-C sample was recycled and used as a regenerated adsorbent for five regeneration cycles (Fig. 11). The adsorption percentage decreases during the five adsorption/desorption cycles. The decrease of the adsorption values can be explained by the progressive loss of crystallinity during the recovery of the precursor material as well as the remaining of certain amounts of diclofenac molecules in the regenerated material [54]. However, the decrease was not too significant, demonstrating the high reusability of the sample, which ascertains its applicability for the removal of diclofenac sodium from aquatic environment.

3.2.10. Suggested adsorption mechanism

The adsorption mechanism was determined by XRD and FTIR analysis. According to the FTIR spectra of the ZnAlFe-CDIC after diclofenac adsorption (Fig. 2), the band at 3,456 cm^{-1} was shifted to 3,426 cm^{-1}, indicating the interaction of diclofenac anions with the hydroxyl groups on adsorbent. New peaks appeared at 1,576, 1,504 and 1,453 cm^{-1} can be ascribed to carboxylate group (COO^-) of diclofenac [35], indicating that diclofenac anions were effectively adsorbed by the adsorbent, implying that some interactions occurred in the process of diclofenac adsorption by the ZnAlFe-C. Furthermore, the XRD pattern of ZnAlFe-CDIC (Fig. 2c) shows characteristic peaks of the original ZnAlFe-CO_3 (Fig. 2a) with a loss in the relative intensity. This effect is due to a decrease in crystallinity,

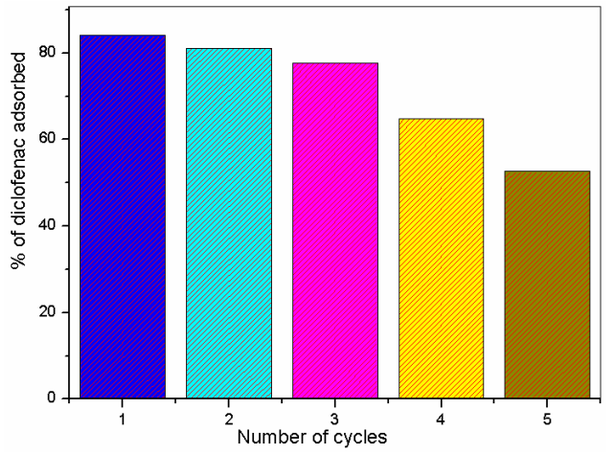

Fig. 11. The results of regeneration test for the adsorption of DIC onto ZnAlFe-C.

caused by the calcination and rehydration of the material. The same observations were reported by Zaghouane et al. [18,19]. Therefore, according to the adsorption experiments and characterization analyses, the removal mechanism of diclofenac ions by ZnAlFe-C is presumed mainly to the so-called "memory effect" [14,15] in which the ZnAlFe-C is rehydrated and the anions of diclofenac are intercalated into the interlayer of the material.

4. Conclusion

The results obtained in this study suggest that ZnAlFe-C is a very efficient anionic adsorbent for diclofenac sorbent and show a high adsorption capacity towards this contaminant. Two adsorption kinetic models were tested and the pseudo second-order model fitted the experimental data adequately. Moreover, the intraparticle diffusion study yielded two linear regions, which suggested that the DIC adsorption involves more than one kinetic stage. The experimental result fits the Langmuir isotherm model well, which suggests that the adsorption process is monolayer. Furthermore, the maximum adsorption capacity for the adsorption of DIC onto ZnAlFe-C was found to be 641.4 mg/g. Owing to its lower price compared to activated carbon , the satisfactorily adsorption results obtained show a promising material for the removal of anionic contaminants in industrial wastewater treatment.

Acknowledgments

Rima Ghemit acknowledges the Laboratory of Chemical Engineering (LGPC) of the University of Sétif, Algeria for the financial support of this work. Special gratitude to Pr. Djellouli Brahim and Pr. Saci Nacef for their technical support.

References

[1] J. Akhtar, N.A.S. Amin, K. Shahzad, A review on removal of pharmaceuticals from water by adsorption, Desal. Water Treat., 57(27) (2016) 12842–12860.

[2] H. Fallou, N. Cimetière, S. Giraudet, D. Wolbert, P. Le Cloirec, Adsorption of pharmaceuticals onto activated carbon fiber cloths-Modeling and extrapolation of adsorption isotherms at very low concentrations, J. Environ. Manage., 166 (2016) 544–555.

[3] M. Graouer-Bacart, S. Sayen, E. Guillon, Adsorption and co-adsorption of diclofenac and Cu(II) on calcareous soils, Ecotoxicol. Environ. Saf., 124 (2016) 386–392.

[4] T. Deblonde, C. Cossu-Leguille, P. Hartemann, Emerging pollutants in wastewater, a review of the literature, Int. J. Hyg. Environ. Health., 214 (2011) 442–448.

[5] Z. Hasan, N.A. Khan, S.H. Jhung, Adsorptive removal of diclofenac sodium from water with Zr-based metal-organic frameworks, Chem. Eng. J., 284 (2016) 1406–1413.

[6] H.R. Busar, T. Poiger, M.D. Müller, Occurrence and fate of the pharmaceutical drug diclofenac in surface waters: rapid photodegradation in a lake, Environ. Sci. Technol., 32 (1998) 3449–3556.

[7] G.R. Boyda, H. Reemtsmaa, D.A. Grimmb, S. Mitrac, Pharmaceuticals and personal care products (PPCPs) in surface and treated waters of Louisiana, USA and Ontario, Canada, Sci. Total Environ., 311 (2003) 135–149.

[8] A. Joss, S. Zabczynski, A. Göbel, B. Hoffmann, D. Löffler, C.S. McArdell, T.A. Ternes, A. Thomsen, H. Siegrist, Biological degradation of pharmaceuticals in municipal wastewater treatment: proposing a classification scheme, Water Res., 40 (2006) 1686–1696.

[9] G.R. Boyd, S. Zhang, D.A. Grimm, Naproxen removal from water by chlorination and biofilm processes, Water Res., 39 (2005) 668–676.

[10] S. Esplugas, D.M. Bila, L. Gustavo, T. Krause, M. Dezotti, Ozonation and advanced oxidation technologies to remove endocrine disrupting chemicals (EDCs) and pharmaceuticals and personal care products (PPCPs) in water effluents, J. Hazard. Mater., 149 (2007) 631–64.

[11] M. Klavarioti, D. Mantzavinos, D. Kassinos, Removal of residual pharmaceuticals from aqueous systems by advanced oxidation processes, Environ. Int., 35 (2009) 402–417.

[12] M. Antunes, V.I. Esteves, R. Guégan, J.S. Crespo, A.N. Fernandes, M. Giovanela, Removal of diclofenac sodium from aqueous solution by isabel grape bagasse, J. Chem. Eng., 192 (2012) 114–121.

[13] R. Baccar, M. Sarrà, J. Bouzid, M. Feki, P. Blánquez, Removal of pharmaceutical compounds by activated carbon prepared-from agricultural by product, Chem. Eng. J., 211–212 (2012) 310– 317.

[14] F. Cavani, F. Trifiro`, A. Vaccari, Hydrotalcite-type anionic clays: Preparation, properties and applications, Catal. Today, 11(2) (1991) 173–301.

[15] I.L. V, J. He, M. Wei, D.G. Evans, X. Duan, Factors influencing the removal of fluoride from aqueous solution by calcined Mg-Al-CO_3 layered double hydroxides. J. Hazard. Mater., 133 (2006) 119–126.

[16] D. Carriazo, del. M. Arco, C. Martin, V. Rives, A comparative study between chloride and calcined carbonate hydrotalcites as adsorbents for Cr(VI), App. Clay. Sci., 37 (2007) 231–239.

[17] C. Geng, T. Xu, Y. Li, Z. Chang, X. Sun, X. Lei, Effect of synthesis method on selective adsorption of thiosulfate by calcined MgAl-layered double hydroxides, J. Chem. Eng., 232 (2013) 510–518.

[18] H. Zaghouane-Boudiaf, M. Boutahala, C. Tiar, L. Arab, F. Garin, Treatment of 2,4,5 trichlorophenol by MgAl–SDBS organo-layered double hydroxides: Kinetic and equilibrium studies, J. Chem. Eng., 173 (2011) 36–41.

[19] H. Zaghouane-Boudiaf, M. Boutahala, L. Arab, Removal of methyl orange from aqueous solution by uncalcined and calcined MgNiAl Layered double hydroxides (LDHs), J. Chem. Eng., 187 (2012) 142–149.

[20] D. Chebli, A. Bouguettoucha, A. Reffas, C. Tiar, M. Boutahala, H. Gulyas, A. Amrane, Removal of the anionic dye Biebrich scarlet from water by adsorption to calcined and non-calcined Mg–Al layered double hydroxides, Desal. Water Treat., 57(46) (2016) 22061–22073.

[21] L. Arab, M. Boutahala, B. Djellouli, T. Dintzer, V. Pitchon, Characteristics of gold supported on nickel-containing hydrotalcite catalysts in CO oxidation, Appl. Catal. A., 475 (2014) 446–460.
[22] L. Arab, M. Boutahala, B. Djellouli, Etude de l'élimination du Cr(VI) par l'oxyde mixte obtenu par calcination de l'hydroxyde double lamellaire MgAl, C. R. Chim., 17 (2014) 860–868.
[23] W.T. Reichle, Synthesis of anionic clay minerals (mixed metal hydroxides hydrotalcite), Solid State Ionics, 22 (1986) 135–141.
[24] S. Brunauer, P.H. Emmett, E. Teller, Adsorption of gases in multimolecular layers, J. Am. Chem. Soc., 60 (1938) 309–319.
[25] E.P. Barrett, L.G. Joyner, P.H. Halenda, The determination of pore volume and area distributions in porous substances. I. Computations from nitrogen isotherms, J. Am. Chem. Soc., 73 (1951) 373–380.
[26] K. El Hassani, B.H. Beakou, D. Kalnina, E. Oukani, A. Anouar, Effect of morphological properties of layered double hydroxides on adsorption of azo dye Methyl Orange: A comparative study, Appl. Clay Sci., 140 (2017)124–131.
[27] C. Tiar, M. Boutahala, A. Benhouria, H. Zaghouane-Boudiaf, Synthesis and physicochemical characterization of ZnMgNiAl-CO_3-layered double hydroxide and evaluation of its sodium dodecylbenzenesulfonate removal efficiency, Desal. Water Treat., 57(28) (2016) 13132–13143.
[28] S. Xia, R. Nie, X. Lu, L. Wang, P. Chen, Z. Hou, Hydrogenolysis of glycerol over $Cu_{0.4}/Zn_{5.6-x}Mg_xAl_2O_{8.6}$ catalysts: The role of basicity and hydrogen spillover, J. Catal., 296 (2012) 1–13.
[29] C. Forano, U. Costantino, C. Taviot-Gueho, Handbook of clay science, In: Bergaya, F. Lagaly, G. (Eds,), Developments in Clay Science. Elsevier, Amsterdam, pp. 745–782.
[30] N. Benselka-Hadj Abdelkader, A. Bentouami, Z. Derriche, N. Bettahar, L.-C. deMénorval, Synthesis and characterization of Mg-Fe layer double hydroxides and its application on adsorption of orange G from aqueous solution, Chem. Eng. J., 169, (2011) 231–238.
[31] M.J. Hernandez-Moreno, M.A. Ulibarri, J.L. Rendon, C.J. Serna, IR characteristics of hydrotalcite-like compounds, Phys. Chem. Miner., 12 (1985) 34–38.
[32] J.T. Kloprogge, R.L. Frost, Fourier transform infrared and Raman spectroscopic study of the local structure of Mg, Ni, and Co-Hydrotalcites, Phys. Chem. Miner., 146 (1999) 506–515.
[33] O.P. Ferreira, O.L. Alves, D.X. Gouveia, A.G.S. Filho, J.A.C. de Paiva, J.M. Filho, Thermal decomposition and structural reconstruction effect on Mg–Fe based hydrotalcite compounds, J. Solid State Chem., 177 (2004) 3058–3069.
[34] M.K. Titulaer, J.B.H. Jansen, J.W. Geus, The quantity of reduced nickel in synthetic takovite: effects of preparation conditions and calcinations temperature, Clays Clay Miner., 42 (1994) 249–258.
[35] F. Caoa, Y. Wanga, Q. Ping, Z. Liao, Zn–Al–NO_3-layered double hydroxides with intercalated diclofenac for ocular delivery, Int. J. Pharm., 404 (2011) 250–256.
[36] J. Zhou, S. Yang, J. Yu, Z. Shu, Novel hollow microspheres of hierarchical zinc–aluminum layered double hydroxides and their enhanced adsorption capacity for phosphate in water, J. Hazard. Mater., 192 (2011) 1114–1121.
[37] Z. Yu, D. Chen, M. Ronning, V. Torbjorn, E. Ochoa-Fernandez, A. Holmen, Large scale synthesis of carbon nanofibers on Ni–Fe–Al hydrotalcite derived catalysts. I. Preparation and characterization of the Ni–Fe–Al hydrotalcites and their derived catalysts, Appl. Catal. A., 338 (2008) 136–146.
[38] H. Wei, S. Deng, Q. Huang, Y. Nie, B. Wang, J. Huang, G. Yu, Regenerable granular carbon nanotubes/alumina hybrid adsorbents for diclofenac sodium and carbamazepine removal from aqueous solution, Water Res., 47 (2013) 4139–4147.
[39] D. Tiwari, C. Lalhriatpuia, S.M. Lee, Hybrid materials in the removal of diclofenac sodium from aqueous solutions: Batch and column studies, J. Ind. Eng. Chem., 30 (2015) 167–173.
[40] S. Sahnoun, M. Boutahala, H. Boudiaf, L. Zerroual, Trichlorophenol removal from aqueous solutions by modified halloysite: Kinetic and equilibrium, Desal. Water. Treat., 57(34) (2016) 15941–15951.
[41] X. Lu, Y. Shao, N. Gao, J. Chen, Y. Zhang, Q. Wang, Y. Lu, Adsorption and removal of clofibric acid and diclofenac from water with MIEX resin, Chemosphere, 161 (2016) 400–411.
[42] A. Benhouria, Md.A. Islam, H. Zaghouane-Boudiaf, M. Boutahala, B.H. Hameed, Calcium alginate-bentonite-activated carbon composite beads as highly effective adsorbent for methylene blue, Chem. Eng. J, 270 (2015) 621–630.
[43] S.Y. Lagergren, Zurtheorie der sogenannten adsorption geloesterstoffe (On the theory of so-called adsorption of solutes), K. Sven. Vetenskapsakad. Handl., 24 (1898) 1–39.
[44] Y.S. Ho, G. McKay, Pseudo-second-order model for sorption processes, Process Biochem., 34 (1999) 451–465.
[45] N. Suriyanon, P. Punyapalakul, C. Ngamcharussrivichai, Mechanistic study of diclofenac and carbamazepine adsorption on functionalized Silica-based porous materials, J. Chem. Eng., 214 (2013) 2018–218.
[46] S.A. Torrellas, A.R. Rodriguez, G.O. Escudero, J.M.G. Martin, J.G. Rodriguez, Comparative evaluation of adsorption kinetics of diclofenac and isoproturon by activated carbon, J. Environ. Sci. Health A: Tox. Hazard. Subst. Environ. Eng., 50 (2015) 1241– 12489.
[47] N. Boukhalfa, M. Boutahala, N. Djebri, Synthesis and characterization of ZnAl-layered double hydroxide and organo-K10 montmorillonite for the removal of diclofenac from aqueous solution, Adsorpt. Sci. Technol., 35(1–2) (2017) 20–36.
[48] W.J. Weber, J.C. Morris, Kinetics of adsorption on carbon from solution, J. Sanitary Eng. Div., 89 (1963) 31–60.
[49] G.E. Boyd, A.W. Adamson, LS. Myers, The exchange adsorption of ions from aqueous solutions by organic zeolites, II. Kinetics, J. Am. Chem. Soc., 69 (1947) 2836–2848.
[50] I. Langmuir, The constitution and fundamental properties of solids and liquids, J. Am. Chem. Soc., 38 (1916) 2221–2295.
[51] H.M.F. Freundlich, Uber die adsorption in loesungen, Z. Phys. Chem. 57 (1906) 385–470.
[52] R. Sips, Combined form of Langmuir and Freundlich equations. J. Chem. Phys., 16 (1948) 490–495.
[53] N. Suriyanon, P. Punyapalakul, C. Ngamcharussrivichai, Mechanistic study of diclofenac and carbamazepine adsorption on functionalized Silica-based porous materials, J. Chem. Eng., 214 (2013) 2018–218.
[54] M.X. Zhu, Y.P. Li, M. Xie, H.Z. Xin, Sorption of an anionic dye by uncalcined and calcined layered double hydroxides: A case study, J. Hazard. Mater., 120 (2005) 163–1741.
[55] S. Larous, A.H. Meniai, Adsorption of diclofenac from aqueous solution using activated carbon prepared from olive stones, Int. J. Hydrogen Energy, 41(24) (2016) 10380–10390.
[56] H. Mabrouki, D.E. Akreche, Diclofenac potassium removal from water by adsorption on natural and pillared clay, Desal. Water Treat., 57(13) (2016) 6033–6043.
[57] C. Saucier, M.A. Adebayo, E.C. Lima, R. Cataluna, P.S. Thue, L.D.T. Prola, M.J. Puchana-Rosero, F.M. Machado, F.A. Pavan, G. Dotto, Microwave-assisted activated carbon from cocoa shell as adsorbent for removal of sodium diclofenac and nimesulide from aqueous effluents, J. Hazard. Mater., 289 (2015) 18–27.
[58] D. Krajisnika, A. Dakovic, M. Milojevic, A. Malenovic, M. Kragovic, D.B. Bogdanovic, V. Dondur, J. Milic, Properties of diclofenac sodium sorption onto natural zeolite modified with cetylpyridinium chloride, Colloids Surf. B: Biointerfaces, 83 (2011) 165–172.
[59] J. Janicijevic, Modified local diatomite as potential functional drug carrier-A model study for diclofenac sodium, Int. J. Pharm., 496 (2015) 466–474.